

Modeling and Robust Adaptive Control of a 3-Axis Motion Simulator

Xie Yue, Mahinda Vilathgamuwa, K. J. Tseng and N. Nagarajan

School of Electrical and Electronic Engineering

Nanyang Technological University

Nanyang Avenue, Singapore 639798.

e-mail: p148881015@ntu.edu.sg, emahinda@ntu.edu.sg, ekjtseng@ntu.edu.sg, enara@ntu.edu.sg

Abstract—In this paper, the development of a 3-axis motion simulator is described. The simulator is used to test and calibrate certain spacecraft instruments within a hardware-in-the-loop environment. A mathematical electromechanical model of the simulator is developed. Moreover, a novel robust adaptive nonlinear control law for the simulator is developed based on Lyapunov stability theory. The controller can be made adaptable to constant unknown parameters as well as robust to unknown but bounded fast varying disturbances. The motion simulator actuators are Permanent Magnet Synchronous Motor (PMSM) drives. The simulation and experimental results are presented to verify the efficacy of the proposed control system and the validity of the mathematical model of the simulator.

I. INTRODUCTION

The instruments used in a spacecraft are mission critical real-time embedded systems, which have to be tested to ensure reliable operation in space [1]-[3]. In order to verify their operative correctness, an end-to-end system testing must be carried out. Towards this end, a 3-axis motion simulator can be used to test the operation of sun sensor, star sensor and other gyroscopic instruments used in a spacecraft within a space-like environment. The motion simulator generates a user defined 3-dimensional motion profile by using 3 PMSM direct drive motors fixed along roll, pitch and yaw axes.

In this paper, the mathematical model of this mechanical structure is derived by means of calculating the angular momentum of each rotating part with respect to its reference frame. A compact mathematical model of the whole electromechanical system is obtained by representing the PMSM motor drives in the field orientation. There are complex nonlinear couplings among three axes in the mathematical model of the simulator, which may degrade the control performance.

In order to realize high performance motion control of this highly nonlinear electromechanical system, the input-output linearization approach can be used [4], [5]. However, in practice, the model of the simulator is usually imprecise. There are uncertainties in motor parameters due to measurement errors and in load inertia due to change of the payload. In order to overcome the effects of parameter uncertainty on controllability of the plant, a few control methods have been proposed, e.g. sliding mode control, adaptive nonlinear control [6]-[12]. However, most of these works concentrate on single motor driven actuator systems in contrast to the proposed system which has 3 axes and is highly nonlinear. The existing complexity of the system can be aggravated with the appearance of more coupling terms in the torque equation if the payload centre of gravity deviates from the intersection point of the three axes. These torque components are in addition to Centripetal and Coriolis torque components, which have already been considered in the modeling process. Despite the presence of these torque components which can be categorized as disturbances, the

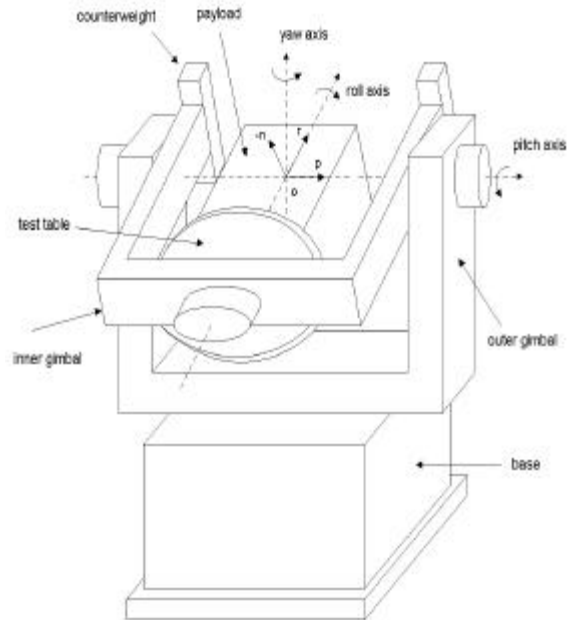


Fig. 1. 3-axis motion simulator

system can be made effectively insensitive to disturbances and parameter variations by adopting a robust adaptive control law. The efficiency and correctness of the proposed control system are verified using simulation results and laboratory experimental results.

II. THE STRUCTURE OF THE 3-AXIS MOTION SIMULATOR AND HARDWARE-IN-THE-LOOP TESTING

The structure of 3-axis motion simulator is shown in Fig. 1. It is comprised of an outer gimbal, an inner gimbal, a test table, three motors, counterweights and a base. The payload is mounted on the top of the test table. The outer gimbal rotates around a vertical yaw axis, it is driven by a motor located inside the base. The inner gimbal moves around a horizontal pitch axis and is driven by another motor, which is fixed on the outer gimbal. The third motor is fixed on the inner gimbal and drives the test table which rotates about the roll axis, which is perpendicular to the pitch axis. The yaw, pitch and roll axes meet at a single point in space. The whole structure is designed to be axi-symmetric. The counterweights fixed in the inner gimbal are used to balance the pay-load such that the center of gravity of the inner gimbal and the payload lies on the pitch axis. The three motors used are PMSM direct drive rotary (DDR) motors,

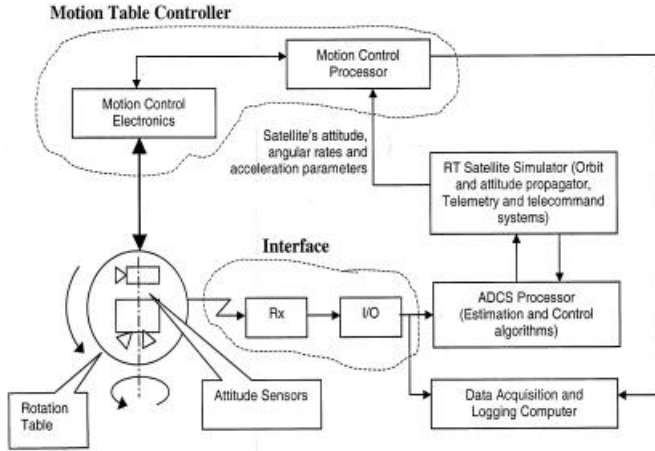


Fig. 2. HWIL Simulation for the satellite ACS systems

which are installed along these three axes and are named roll, pitch and yaw motors respectively.

Primarily there are two kinds of 3-axis motion platforms. The first platform is 3-axis air bearing with sensors, actuators, and control electronics mounted on it. The second is 3-axis servo table platform for sensors with control electronics and actuators outside the platform, and the control loop is closed through a digital computer that simulates satellite dynamics and in turn drives the servo table. Air bearing simulations are the most common throughout the space industry for testing the satellite Attitude Control System (ACS) as it is easy to implement. However, it has many shortcomings for precise evaluation of the performance due to undesirable air bearing torques comparable to control torques and difficulties in simulating actual satellite inertia. In recent times, precise servo table simulations have become more common [3].

A block diagram of Hardware-in-the-loop (HWIL) simulation for the satellite ACS systems is shown in Fig. 2. The main components of HWIL simulation include rotation table, motion table controller, sensors, data acquisition and Real Time (RT) simulator.

This rotation table, namely motion simulator is used for mounting and calibrating the performance of attitude sensors (like sun, star sensors, and gyros). The motion table controller includes motion control processor and electronics, it is driven by track inputs, *i.e.* satellite's attitude, angular rates and angular acceleration, from the satellite RT simulator. Sensors measure the attitude signals excited by the rotation table and, through sensors-flight control processor interface, provide the outputs to ACS computer for RT simulation. Data acquisition processor logs in the data from sensors, motion controller, and motion table for post analysis. The satellite dynamics are simulated in real-time, based on a mathematical model of the space environment, which includes atmospheric drag, solar radiation pressure and magnetic field, the satellite rigid body dynamics and certain additional ACS components. The satellite position, rate and acceleration calculated from the

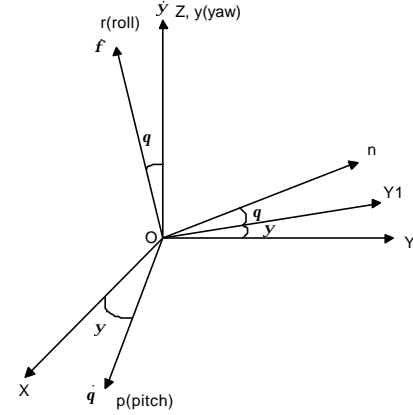


Fig. 3. Axial representation of motion simulator based on classical Euler angles

simulated satellite behavior in space are fed to motion controller and they are used to drive the motion simulator to excite those optical and inertial attitude sensors.

III. DYNAMIC MECHANICAL MODEL OF 3-AXIS MOTION SIMULATOR

The simulator has three rotating parts, namely roll part including payload and test table; pitch part including inner gimbal, counterweights and roll motor; and yaw part including outer gimbal and pitch motor. As shown in Fig. 3, angles f , q and y are denoted as roll, pitch and yaw angles respectively and measured from their initial states. Accordingly, the angular velocities about these three axes are $w_r(f)$, $w_p(q)$ and $w_y(y)$. Note that n is perpendicular to rp plane. The angular velocity of rpn frame fixed on the inner gimbal is,

$$\begin{aligned} \vec{w}^{rpn} &= \vec{w}_p + \vec{w}_y \\ &= w_p \mathbf{p} + w_y \cos q \mathbf{r} + w_y \sin q \mathbf{n} \end{aligned} \quad (1)$$

The angular velocities of the simulator about three axes expressed in rpn frame are,

$$\begin{aligned} \vec{w}_r &= w_r \mathbf{r}, \quad \vec{w}_p = w_p \mathbf{p} \\ \vec{w}_y &= w_y \cos q \mathbf{r} + w_y \sin q \mathbf{n} \end{aligned} \quad (2)$$

The angular momentum of the roll part is,

$$\vec{H}_r = I_r (\vec{w}_r + \vec{w}_p + \vec{w}_y) \quad (3)$$

where the roll part is assumed to be axi-symmetric, and its constant moment of inertia matrix is of the form $I_r = \text{diag}[I_{rr}, I_{rpn}, I_{rpn}]$ in the rpn frame. Therefore the external torque \vec{M}_r^i acting on the roll part is,

$$\begin{aligned} \vec{M}_r^i &= \dot{\vec{H}}_r^{rpn} + \vec{w}^{rpn} \times \vec{H}_r \\ &= M_{rr} \mathbf{r} + M_{rp} \mathbf{p} + M_{rn} \mathbf{n} \end{aligned} \quad (4)$$

where M_{rr} is produced by the roll motor, while M_{rp} and M_{rn} are acting as transverse forces on the bearings,

which connect the shaft of the inner motor. Combining (1) with (4), we have,

$$M_{rr} = \ddot{\mathbf{f}}_{rr} + (\ddot{\mathbf{y}} \cos \mathbf{q} - \dot{\mathbf{y}} \dot{\mathbf{q}} \sin \mathbf{q}) I_{rr} \quad (5)$$

Similarly, the angular momentums of the pitch part and yaw are given by

$$\bar{H}_p = \bar{H}_r + I_p (\bar{\mathbf{w}}_p + \bar{\mathbf{w}}_y) \quad (6)$$

$$\bar{H}_y = \bar{H}_p + I_{yy} \bar{\mathbf{w}}_y \quad (7)$$

where constant moment of inertia matrix of the pitch part is $I_p = \text{diag}[I_{pr}, I_{pp}, I_{pn}]$ and I_{yy} is yaw part moment of inertia about the yaw axis.

The rotation matrix from **rpn** frame to the inertia frame is given by

$$R^{irpn}(\mathbf{y}, \mathbf{q}) = \begin{bmatrix} c\mathbf{y} & s\mathbf{y}c\mathbf{q} & s\mathbf{y}s\mathbf{q} \\ s\mathbf{y} & c\mathbf{y}c\mathbf{q} & c\mathbf{y}s\mathbf{q} \\ 0 & s\mathbf{q} & c\mathbf{q} \end{bmatrix} \quad (8)$$

where c indicates cosine and s indicates sine. Using a formation similar to (4), we can obtain the external torque components \bar{M}_p^i and \bar{M}_y^i , which act on the pitch part and yaw part, in **rpn** frame and inertia frame respectively. Among these torque components, we have

$$M_{pp} = (I_{rpn} + I_{pp}) \ddot{\mathbf{q}} + I_{rr} \ddot{\mathbf{f}} \dot{\mathbf{y}} s \mathbf{q} + (I_{rr} + I_{pr} \quad I_{rpn} \quad I_{pn}) \dot{\mathbf{y}}^2 s \mathbf{q} c \mathbf{q} \quad (9)$$

$$M_{yz} = (I_{yy} + I_{rpn} + I_{pn}) \ddot{\mathbf{y}} + I_{rr} (\ddot{\mathbf{f}} c \mathbf{q} \quad \dot{\mathbf{f}} \dot{\mathbf{q}} s \mathbf{q}) + (I_{rr} + I_{pr} \quad I_{rpn} \quad I_{pn}) \dot{\mathbf{y}} c^2 \mathbf{q} \quad \dot{\mathbf{y}} \dot{\mathbf{q}} s 2 \mathbf{q} \quad (10)$$

where M_{pp} and M_{yz} are produced by the pitch and yaw motors respectively.

The mathematical model of the motion simulator can be obtained by combining (5), (9) and (10):

$$\mathbf{t} - T_f = M \quad (11)$$

where $\mathbf{t} = [T_{emr} \quad T_{emp} \quad T_{emy}]^T$ is demanded torque vector of the three motors; $M = [M_{rr} \quad M_{pp} \quad M_{yz}]^T$ is the load torque vector. Disturbance torque vector $T_f = [T_{fr} \quad T_{fp} \quad T_{fy}]^T$ is comprised of friction, external disturbances and additional coupling torques due to unstructured uncertainties in modeling process, e.g. moment of inertia matrix I_r being not diagonal because of the payload's uncertainty, both in its shape and location on the test table and the non-orthogonality of yaw and roll axes about the pitch axis.

The mathematical model (11) gives the relationships between motor torques and rotational angles about three axes, which are directly associated with the payload's attitude variables expressed with *Euler's* angles [13]. This makes it convenient to control the motion simulator within a satellite based reference frame.

IV. MATHEMATICAL MODEL OF ELECTROMECHANICAL SYSTEM

In synchronous d - q rotor reference frame, the PMSM motor equations can be written as,

$$\begin{aligned} u_{di} &= R_i i_{di} + L_{di} \dot{i}_{di} - L_{qi} P_i i_{qi} \omega_i \\ u_{qi} &= R_i i_{qi} + L_{qi} \dot{i}_{qi} + L_{di} P_i i_{di} \omega_i + P_i I_i \omega_i \\ T_{emi} &= \frac{3}{2} P_i [(L_{di} - L_{qi}) i_{di} i_{qi} + I_i i_{qi}] \end{aligned} \quad (12)$$

where $i = r, p, y$ (r, p, y denote roll, pitch and yaw motors); u_{di}, u_{qi} are stator voltages; R_i, L_{di} and L_{qi} represent stator resistance and motor d and q axis inductances; i_{di}, i_{qi} are d and q axis currents; I_i is flux linkage of the rotor magnet; ω_i, P_i and T_{emi} are rotor speed, number of pole pairs and electromagnetic torque of the motor respectively.

Rearranging (11), we have

$$H(q) \ddot{\mathbf{q}} + C(q, \dot{\mathbf{q}}) \dot{\mathbf{q}} + T_f = \mathbf{t} \quad (13)$$

where $\mathbf{q} = [\mathbf{f} \quad \mathbf{q} \quad \mathbf{y}]^T$ is the position vector. $H(q)$ is the simulator inertia matrix which is a symmetric positive definite matrix.

$$\begin{aligned} H(q) &= \begin{bmatrix} I_1 & 0 & I_1 c \mathbf{q} \\ 0 & I_2 & 0 \\ I_1 c \mathbf{q} & 0 & I_4 + I_3 c^2 \mathbf{q} \\ 0 & I_1 \dot{\mathbf{y}} s \mathbf{q} & 0 \end{bmatrix} \\ C(q, \dot{\mathbf{q}}) &= \begin{bmatrix} I_1 \dot{\mathbf{y}} s \mathbf{q} & 0 & I_3 \dot{\mathbf{y}} s \mathbf{q} c \mathbf{q} \\ I_1 \dot{\mathbf{q}} s \mathbf{q} & I_3 \dot{\mathbf{y}} s \mathbf{q} c \mathbf{q} & I_3 \dot{\mathbf{q}} s \mathbf{q} c \mathbf{q} \end{bmatrix} \\ I_1 &= I_{rr}; \quad I_2 = I_{rpn} + I_{pp} \\ I_3 &= I_{rr} + I_{pr} \quad I_{rpn} \quad I_{pn}; \\ I_4 &= I_{yy} + I_{rpn} + I_{pn} \end{aligned}$$

The mathematical model of the electromechanical system can be obtained by combining (12) and (13) as

$$\begin{bmatrix} A_d & 0 & 0 & F_d & 1 & 0 & 0 \\ 0 & A_q & 0 & F_q & + & 0 & 1 & 0 & u \\ 0 & 0 & H & C \dot{\mathbf{q}} & T_f + \mathbf{t} & 0 & 0 & 0 \end{bmatrix} \dot{\mathbf{x}} = \mathbf{x} \quad (14)$$

where

$$A_d = \begin{bmatrix} L_{dr} & 0 & 0 \\ 0 & L_{dp} & 0 \\ 0 & 0 & L_{dy} \end{bmatrix}, \quad A_q = \begin{bmatrix} L_{qr} & 0 & 0 \\ 0 & L_{qp} & 0 \\ 0 & 0 & L_{qy} \end{bmatrix}$$

$$\mathbf{x} = [i_d \quad i_q \quad \mathbf{w}]^T, \quad \mathbf{x} \in R^9$$

$$i_d = [i_{dr} \quad i_{dp} \quad i_{dy}]^T, \quad i_q = [i_{qr} \quad i_{qp} \quad i_{qy}]^T, \quad \mathbf{w} = \dot{\mathbf{q}}$$

$$\mathbf{u} = [u_d \quad u_q \quad 0]^T, \quad \mathbf{u} \in R^9$$

$$u_d = [u_{dr} \quad u_{dp} \quad u_{dy}]^T$$

$$u_q = [u_{qr} \quad u_{qp} \quad u_{qy}]^T$$

$$F_d = [f_{dr} \quad f_{dp} \quad f_{dy}]^T$$

$$F_q = [f_{qr} \quad f_{qp} \quad f_{qy}]^T$$

$$\begin{aligned} f_{di} &= R_i \dot{i}_{di} + L_{qi} P_i \dot{i}_{qi} \mathbf{w}_i \\ f_{qi} &= R_i \dot{i}_{qi} - L_{di} P_i \dot{i}_{di} \mathbf{w}_i - P_i \mathbf{I}_i \mathbf{w}_i \end{aligned}$$

By differentiating (13), the input-output linearization of MIMO system (14) can be carried out as follows,

$$\begin{aligned} & \begin{bmatrix} A_d & 0 \\ 0 & H \end{bmatrix} \begin{bmatrix} \dot{i}_d \\ \ddot{q} \end{bmatrix} \\ &= \begin{bmatrix} \dot{H} + C \\ \dot{C} \end{bmatrix} \ddot{q} + \begin{bmatrix} F_d \\ \dot{T}_f + BF_d + DF_q \end{bmatrix} + \begin{bmatrix} 1 & 0 \\ B & D \end{bmatrix} \begin{bmatrix} u_d \\ u_q \end{bmatrix} \end{aligned} \quad (15)$$

where B and D are diagonal matrices and are described by

$$\begin{aligned} B &= \begin{bmatrix} a_r i_{qr} / L_{dr} & 0 & 0 \\ 0 & a_p i_{qp} / L_{dp} & 0 \\ 0 & 0 & a_y i_{qy} / L_{dy} \end{bmatrix} \\ D &= \begin{bmatrix} (a_i i_{dr} + b_r) / L_{qr} & 0 & 0 \\ 0 & (a_j i_{dp} + b_p) / L_{qp} & 0 \\ 0 & 0 & (a_k i_{dy} + b_y) / L_{qy} \end{bmatrix} \end{aligned}$$

$$a_i = \frac{3}{2} P_i (L_{di} \quad L_{qi}), b_i = \frac{3}{2} P_i \mathbf{I}_i$$

As the total relative degree is the same as the order of the system (14), there is no internal dynamics.

V. ROBUST ADAPTIVE NONLINEAR TRACKING CONTROL DESIGN

Now the control task is to get the output \mathbf{q} to track a specific time-varying 9-dimensional vector, $\mathbf{q} = [q \quad \dot{q} \quad \ddot{q}]^T$, i.e. a desired trajectory based on satellite attitude dynamics. Assume motor parameters and simulator's moment of inertia matrices are unknown, disturbance vector T_f is unknown but has known bounds.

For the outputs i_d and q of the system (14), two sliding surfaces s_1 and s_2 are defined as follows,

$$s_1 = \left(\frac{d}{dt} + \mathbf{I}_1 \right) \int_0^t \tilde{i}_d dt \quad (16)$$

$$s_2 = \left(\frac{d}{dt} + \mathbf{I}_2 \right)^2 \tilde{q} \quad (17)$$

where $\tilde{i}_d = i_d - i_{d_d}$, $\tilde{q} = q - q_d$; i_{d_d} and q_d are reference values of i_d and q ; \mathbf{I}_1 and \mathbf{I}_2 are strictly positive constant diagonal matrices.

In order to select a suitable Lyapunov function for entire system and therefore to obtain a suitable control law, the following two functions are defined,

$$V_1(t) = \frac{1}{2} s_1^T A_d s_1 \quad (18)$$

$$V_2(t) = \frac{1}{2} s_2^T H s_2 \quad (19)$$

where A_d and $H(q)$ are symmetric positive definite matrices. Differentiating both sides of (18) and (19), and using (15), yields

$$\dot{V}_1(t) = s_1^T \begin{bmatrix} 3 \\ Y_i a_i + u_d \end{bmatrix} \quad (20)$$

$$\dot{V}_2(t) = s_2^T \begin{bmatrix} 6 \\ Y_i a_i \quad \dot{T}_f + D u_q \end{bmatrix} \quad (21)$$

where $Y_1 \sim Y_6$ are known matrices based on $i_d, \dot{i}_q, \dot{i}_d, \mathbf{q}, \dot{\mathbf{q}}, \dot{i}_d$ and \ddot{q} (see the Appendix). Y_6 contains u_d and is assumed to be known as it is based on (22). $a_1 \sim a_6$ are parameter vectors of uncertain parameters and their combinations,

$$\begin{aligned} a_1 &= [R_r \quad R_p \quad R_y]^T, a_2 = [L_{qr} \quad L_{qp} \quad L_{qy}]^T \\ a_3 &= [L_{dr} \quad L_{dp} \quad L_{dy}]^T, a_4 = [I_1 \quad I_2 \quad I_3 \quad I_4]^T \\ a_5 &= [a_{5r} \quad a_{5p} \quad a_{5y}]^T, a_5 = R^{18}, a_{5i} = R^6 \end{aligned}$$

$$a_{5i_1} = \left(\frac{L_{qi}}{L_{di}} \quad \frac{L_{di}}{L_{qi}} \right) R_r, a_{5i_2} = \frac{\mathbf{I}_i}{L_{qi}} R_i$$

$$a_{5i_3} = \frac{(L_{di} \quad L_{qi})}{L_{di}} L_{qi}, a_{5i_4} = \frac{(L_{di} \quad L_{qi})}{L_{qi}} L_{di}$$

$$a_{5i_5} = \frac{(2L_{di} \quad L_{qi})}{L_{qi}} \mathbf{I}_i, a_{5i_6} = \frac{\mathbf{I}_i^2}{L_{qi}}$$

$$a_6 = \left[\frac{(L_{dr} \quad L_{qr})}{L_{dr}}, \frac{(L_{dp} \quad L_{qp})}{L_{dp}}, \frac{(L_{dy} \quad L_{qy})}{L_{dy}} \right]^T$$

Taking the control law to be

$$u_d = Y_1 \hat{a}_1 + Y_2 \hat{a}_2 + Y_3 \hat{a}_3 - K_{D1} s_1 \quad (22)$$

$$u_q = \hat{D}^{-1} \begin{bmatrix} 6 \\ Y_i \hat{a}_i \quad K_{D2} s_2 \quad K_{D3} \text{sgn}(s_2) \end{bmatrix} \quad (23)$$

where K_{D1} and K_{D2} are constant positive definite diagonal matrices; K_{D3} is a positive diagonal matrix; $\hat{a}_j (j=1 \sim 6)$ and \hat{D} are the estimated parameter matrices.

By substituting the control law in (20) and (21), we have

$$\dot{V}_1(t) = s_1^T \begin{bmatrix} 3 \\ Y_i \tilde{a}_i \quad K_{D1} s_1 \end{bmatrix} \quad (24)$$

$$\begin{aligned} \dot{V}_2(t) &= s_2^T \begin{bmatrix} 6 \\ Y_i \tilde{a}_i + \tilde{D} \hat{D}^{-1} \begin{bmatrix} 6 \\ Y_i \hat{a}_i \quad K_{D2} s_2 \\ K_{D3} \text{sgn}(s_2) \end{bmatrix} \end{bmatrix} \\ &= s_2^T \begin{bmatrix} 6 \\ Y_i \tilde{a}_i \quad K_{D2} s_2 \quad K_{D3} \text{sgn}(s_2) \end{bmatrix} \end{aligned} \quad (25)$$

where the known function $K_{D3}(j, j) = |\dot{T}_{fi}|$, ($j=1, i=r$; $j=2, i=p$; $j=3, i=y$), thus K_{D3} can be used to compensate time-variable disturbances. Parameter estimated error $\tilde{a}_i = \hat{a}_i - a_i$.

Note that D is a diagonal matrix, we have

$$\tilde{D} \hat{D}^{-1} \begin{bmatrix} 6 \\ Y_i \hat{a}_i \quad K_{D2} s_2 \quad K_{D3} \text{sgn}(s_2) \end{bmatrix} = Y_7 \tilde{a}_7 + Y_8 \tilde{a}_8 \quad (26)$$

where Y_7 and Y_8 are known matrices (see the Appendix).

Parameter vectors a_7 and a_8 are given by,

$$a_7 = \begin{bmatrix} \frac{L_{dr}}{L_{qr}} & \frac{L_{qp}}{L_{qp}} & \frac{L_{dy}}{L_{qy}} \\ \frac{L_{dr}}{L_{qr}} & \frac{L_{qp}}{L_{qp}} & \frac{L_{dy}}{L_{qy}} \end{bmatrix}^T$$

$$a_8 = \begin{bmatrix} \frac{I_r}{L_{qr}} & \frac{I_p}{L_{qp}} & \frac{I_y}{L_{qy}} \end{bmatrix}^T$$

Now let Lyapunov function candidate to be

$$V(t) = \frac{1}{2} [s_1^T A_d s_1 + s_2^T H s_2 + \sum_{i=1}^8 \tilde{a}_i^T \Gamma_i^{-1} \tilde{a}_i] \quad (27)$$

where Γ_i is a symmetric positive definite matrix.

Differentiating (27) and using (24) and (25), we have,

$$\dot{V}(t) = s_1^T \left[\sum_{i=1}^3 Y_i \tilde{a}_i - K_{D1} s_1 \right] + s_2^T \left[\sum_{i=4}^8 Y_i \tilde{a}_i - \dot{T}_f - K_{D2} s_2 - K_{D3} \text{sgn}(s_2) \right] + \sum_{i=1}^8 \tilde{a}_i^T \Gamma_i^{-1} \dot{\tilde{a}}_i \quad (28)$$

The parameter estimation update rules can be described as follows

$$\dot{\tilde{a}}_i = -\Gamma_i Y_i^T s_1, \quad i = 1, 2, 3 \quad (29)$$

$$\dot{\tilde{a}}_i = -\Gamma_i Y_i^T s_2, \quad i = 4, 5, 6, 7, 8 \quad (30)$$

Thus, we have

$$\dot{V}(t) \leq -s_1^T K_{D1} s_1 - s_2^T K_{D2} s_2 \leq 0 \quad (31)$$

This means that system output errors converge to the sliding surfaces $s_1 = 0$ and $s_2 = 0$ as defined in (16) and (17). Moreover \hat{a}_i is bounded. Therefore, both global stability of the system and convergence of the tracking error are guaranteed by the developed robust adaptive control law.

VI. SIMULATION RESULTS

The performance of the developed control law is investigated with respect to tracking error and robustness using computer simulations.

The desired trajectories are $y_i = A_i \sin(\omega_i t)$ and their derivatives, where $y = \mathbf{f}, \mathbf{q}$ and \mathbf{y} ; $A_i = 0.1 \text{ rad}$; $\omega_r = 2.0 \text{ rad/s}$; $\omega_p = 1.5 \text{ rad/s}$; $\omega_y = 1.0 \text{ rad/s}$, and $i_d = 0$.

Also assume the initial positions and velocities are $\mathbf{f}(0) = 0.3 \text{ rad}$; $\mathbf{q}(0) = 0.2 \text{ rad}$; $\mathbf{y}(0) = 0.1 \text{ rad}$; $\dot{\mathbf{f}}(0) = 0.3 \text{ rad/s}$; $\dot{\mathbf{q}}(0) = 0.2 \text{ rad/s}$; $\dot{\mathbf{y}}(0) = 0.1 \text{ rad/s}$ and the initial accelerations are zero. A constant disturbance $T_f = [10 \ 20 \ 20]^T \text{ Nm}$ is introduced at $t = 5 \text{ s}$ and it lasts for 1 s .

Actual plant and control parameters used in the simulation are listed in the Appendix.

The output \mathbf{q} track the desired trajectories \mathbf{q} as shown in Fig. 4 to Fig.7.

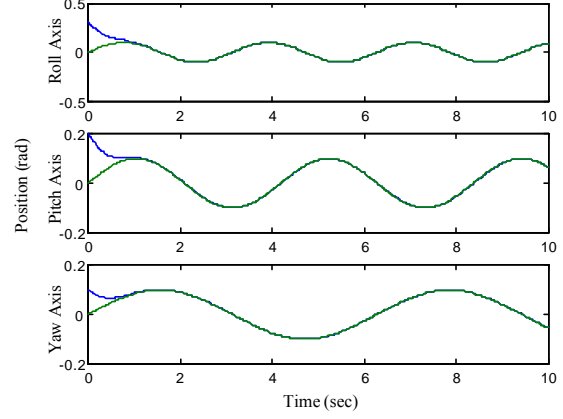


Fig. 4. Three axes position tracking

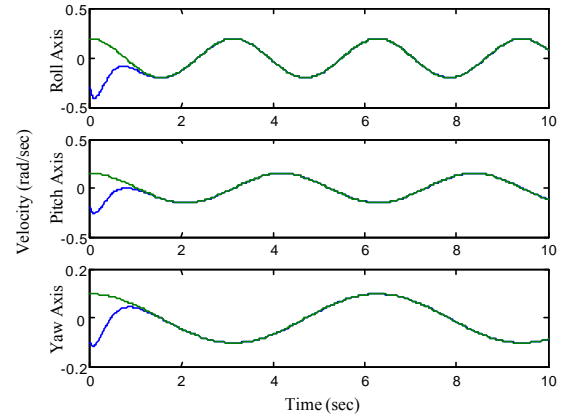


Fig. 5. Three axes velocity tracking

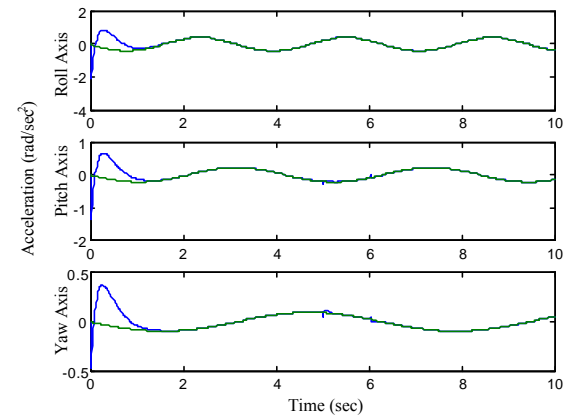


Fig. 6. Three axes acceleration tracking

Simulation results show that the simulator can track the desired trajectories about three axes perfectly, even with disturbances and parameter uncertainty.

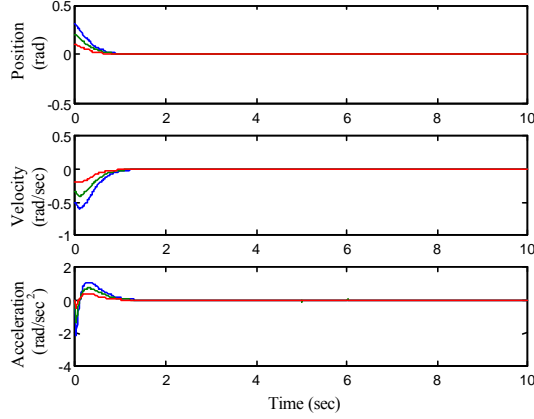


Fig. 7. Three axes tracking error vectors $\tilde{q}, \tilde{\dot{q}}, \tilde{\ddot{q}}$

VII. EXPERIMENTAL RESULTS

Initial laboratory experiments are carried out on a single-axis PMSM motor drive system, using a 32-bit floating-point TMS320C31 digital signal processor (DSP) based motion controller. The block diagram of the experiment system is shown in Fig. 8. As this is a single-axis drive system, the parameters of the robust adaptive control law developed for 3-axis motor drive system should be modified. The control laws with modified parameters for the single-axis system are as follows:

$$u_d = Y_1 \hat{a}_1 + Y_2 \hat{a}_2 + Y_3 \hat{a}_3 \quad K_{D1} s_1 \quad (32)$$

$$u_q = \hat{D}^{-1} \left[\sum_{i=1}^6 Y_i \hat{a}_i \quad K_{D2} s_2 \quad K_{D3} \text{sgn}(s_2) \right] \quad (33)$$

$$\dot{\hat{a}}_i = \sum_{i=1}^4 Y_i^T s_1, \quad i = 1, 2, 3 \quad (34)$$

$$\dot{\hat{a}}_i = \sum_{i=4}^8 Y_i^T s_2, \quad i = 4, 5, 6, 7, 8 \quad (35)$$

where parameters $a_1 \sim a_8$ and $Y_1 \sim Y_8$ have forms similar to their respective counterparts in the 3-axis system. (see Appendix). The only exception is Y_4 , which is associated with coupling issues. However, the robust adaptive control law of the single-axis motor system is similar to that of the 3-axis motor drive system. Therefore preliminary investigation on the performance of the proposed control law can be carried out using the single-axis drive system

The 4-pole permanent magnet synchronous motor shaft is directly coupled to a position sensor and a dynamometer which is used as a programmable load. The motor is supplied by a three-phase voltage-source PWM inverter with a switching frequency of 5 kHz.

Actual motor parameters, their initial estimated values and control parameters are listed in the Appendix.

The desired trajectories are $\mathbf{q} = 40 \sin(0.3t)$ and its derivatives and $i_d = 0$. Assume that the initial position $\mathbf{q}(0) = 0.0$ rad and the motor is initially at standstill. That means initial velocity error $\dot{\mathbf{q}}(0) = 12$ rad/s.

Position, velocity and acceleration have a well-defined relationship. Therefore, velocity and acceleration can be

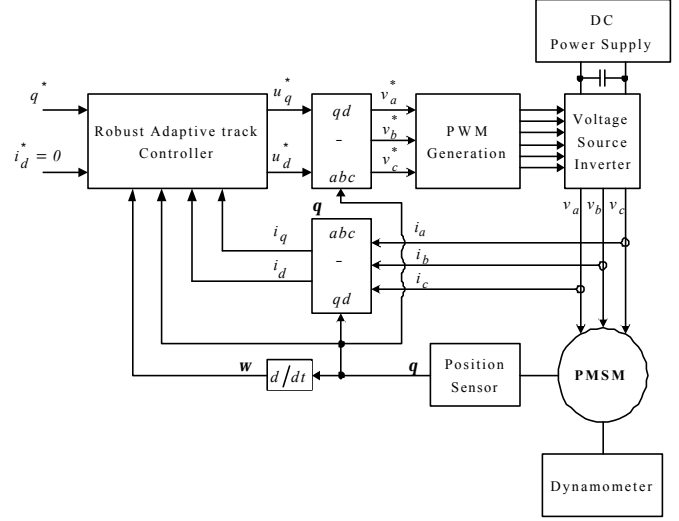


Fig. 8. The block diagram of the experiment system

derived from position signal measured by a high-resolution encoder. A lowpass filter is used for acceleration calculation. A third order Butterworth filter is used for this purpose and the cut-off frequency is 5 rad/s.

Fig. 9 shows the motor shaft position, velocity and acceleration tracking the desired trajectories. Fig. 10 shows the control voltages u_d and u_q . The motor control system begins tracking at time $t = 0$ s. After lapse of few seconds, output \mathbf{q} starts following the desired trajectories

\mathbf{q} satisfactorily. At $t = 36$ s, a constant positive disturbance torque $T_f = 0.6$ Nm is introduced by the dynamometer and it lasts 12 s. Fig. 11 shows an expanded view of the motor output \mathbf{q} . The currents i_d and i_q are shown in Fig.12. The control voltages and currents are modified during the disturbance but position, velocity and acceleration trackings are unaffected. This shows the efficacy of the proposed control law.

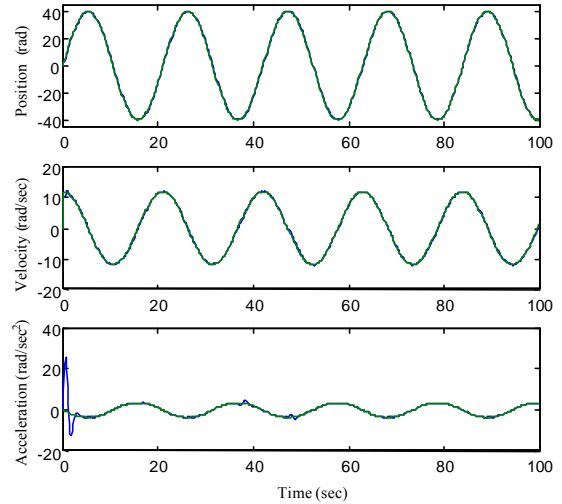


Fig. 9. Position, velocity and acceleration tracking

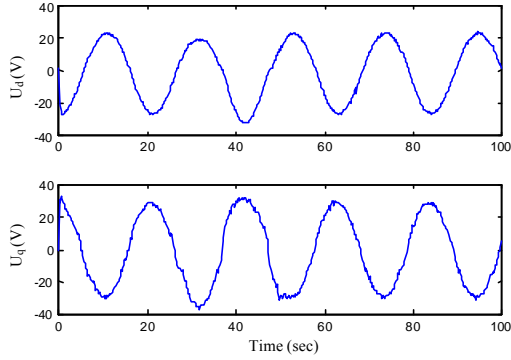


Fig. 10. Control voltages u_d and u_q

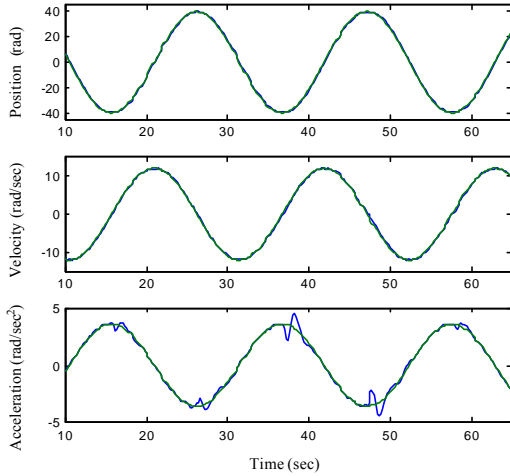


Fig. 11. Position, velocity and acceleration tracking

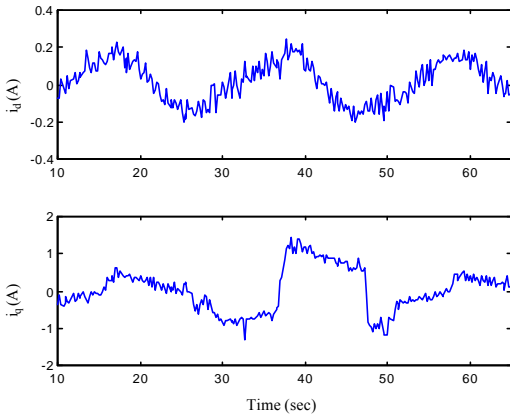


Fig. 12. Currents i_d and i_q

VIII. CONCLUSIONS

The electromechanical model of a 3-axis motion simulator is developed in this paper. Subsequently, using Lyapunov stability method, a robust-adaptive control law, which adapts to constant unknown parameters and behaves robustly against unknown but bounded fast varying disturbances, is

developed. The results obtained from simulations have proven the accuracy and effectiveness of the proposed control law. Preliminary experiments have been carried out using a single-axis drive system to show the efficacy of the proposed control system. The experiment results have proven the correctness and robustness of the control law.

APPENDIX

1. Actual plant parameters used in the simulation are $P_i = 3$, $R_i = 0.513$, $L_{di} = 4.74mH$, $L_{qi} = 9.51mH$,

$$\mathbf{I}_i = 1.278Wb \times \text{turn}, i = r, p, y;$$

$$I_1 = 3.3Kg \times m^2, I_2 = 57.2Kg \times m^2$$

$$I_3 = 45.0Kg \times m^2, I_4 = 154.3Kg \times m^2$$

Initial estimated parameters are

$$I_1 = I_2 = I_3 = I_4 = 0,$$

$$R_i = 0.1, L_{di} = L_{qi} = 0.1mH, \mathbf{I}_i = 0.1Wb \times \text{turn}$$

Control parameters are chosen as

$$\mathbf{I}_1(j, j) = 1, \mathbf{I}_2(j, j) = 2; K_{D3}(i, j) = 0, i = 1, 2, 3; j = 1, 2, 3$$

$$K_{D1} = \text{diag}[400, 300, 300]; K_{D2} = \text{diag}[1000, 800, 700];$$

$\mathbf{I}_i (i = 1 \sim 8)$ is the identity matrix.

2. Parameters of the PMSM motor used in the experiment are $P = 2$, $R = 17.1$, $L_d = 0.278H$, $L_{qi} = 0.369H$,

$$\mathbf{I} = 1.21Wb \times \text{turn}, J = 8.37e^{-3}Kg \times m^2,$$

$$V_{rated} = 400V, f_{rated} = 50Hz.$$

Initial estimated parameters are

$$J = 0.1Kg \times m^2, R_i = 0.1, L_{di} = L_{qi} = 0.1mH,$$

$$\mathbf{I}_i = 0.1Wb \times \text{turn}$$

Control parameters are chosen as

$$\mathbf{I}_1 = 5, \mathbf{I}_2 = 8; K_{D1} = 10, K_{D2} = 1, K_{D3} = 0.01;$$

$$\mathbf{I}_i = 1e^{-4}, (i = 1 \sim 6); \mathbf{I}_i = 1e^{-5}, (i = 7 \sim 13).$$

3. Matrices $Y_1 \sim Y_8$ for the 3-axis motion system are

$$Y_1 = \begin{bmatrix} i_{dr} & 0 & 0 & i_{qr}P_r\dot{\mathbf{f}} & 0 & 0 \\ 0 & i_{dp} & 0 & 0 & i_{qp}P_p\dot{\mathbf{q}} & 0 \\ 0 & 0 & i_{dy} & 0 & 0 & i_{qy}P_y\dot{\mathbf{y}} \end{bmatrix},$$

$$Y_2 = \begin{bmatrix} i_{drr} & 0 & 0 \\ 0 & i_{drp} & 0 \\ 0 & 0 & i_{dry} \end{bmatrix},$$

$$Y_3 = \begin{bmatrix} i_{dri} = \dot{i}_{di} & \mathbf{I}_1(i_d \ i_d) \end{bmatrix}$$

For matrix Y_4 , the non-zero components are listed below:

$$Y_4(1,1) = \ddot{q}_{r1r} + \ddot{q}_{r1y}c\mathbf{q} \quad \ddot{q}_{rp}\dot{\mathbf{y}}s\mathbf{q} \quad \dot{\mathbf{y}}\dot{\mathbf{q}}^2c\mathbf{q} \quad 2\mathbf{I}_{11}(\dot{\mathbf{f}} + \dot{\mathbf{y}}c\mathbf{q})$$

$$2\dot{\mathbf{q}}\dot{\mathbf{y}}s\mathbf{q}$$

$$Y_4(2,1) = \ddot{q}_{rr}\dot{\mathbf{y}}s\mathbf{q} + \dot{\mathbf{f}}\dot{\mathbf{q}}\dot{\mathbf{y}}c\mathbf{q} + \dot{\mathbf{f}}\dot{\mathbf{y}}s\mathbf{q}$$

$$Y_4(3,1) = \ddot{q}_{r1r}c\mathbf{q} \quad \ddot{q}_{rr}\dot{\mathbf{q}}s\mathbf{q} \quad \dot{\mathbf{f}}\dot{\mathbf{q}}^2c\mathbf{q} \quad 2\mathbf{I}_{33}\ddot{c}\mathbf{q} \quad \dot{\mathbf{q}}\dot{\mathbf{f}}s\mathbf{q} \quad \dot{\mathbf{f}}\dot{\mathbf{q}}s\mathbf{q}$$

$$Y_4(2,2) = \ddot{q}_{r1p} \quad 2\mathbf{I}_{22}\ddot{\mathbf{q}}$$

$$Y_4(2,3) = \ddot{q}_{r1} \dot{y} s q c q + \dot{y}^2 \dot{q} c^2 q + \dot{y} \ddot{y} s q c q$$

$$Y_4(3,3) = \ddot{q}_{r1y} c^2 q - (\ddot{q}_{rp} \dot{y} + \ddot{q}_{ry} \dot{q}) s q c q + 2 \dot{y} \dot{q}^2 c^2 q$$

$$2 I_{33} \dot{y} c^2 q - \dot{y} \ddot{q} s q c q - 3/2 * \dot{q} \dot{y} s^2 q$$

$$Y_4(3,4) = \ddot{q}_{r1y} - 2 I_{23} \ddot{y}$$

$$\ddot{q}_r = \ddot{q} - 2 I_2 \ddot{\tilde{q}} - I_2^2 \ddot{\tilde{q}}$$

$$\ddot{q}_{r1} = \ddot{q} + 2 I_2 \ddot{\tilde{q}} - I_2^2 \ddot{\tilde{q}}$$

$$\ddot{\tilde{q}} = \ddot{q} - \ddot{q}$$

$$Y_{5r} = 0 \quad 0$$

$$Y_5 = 0 \quad Y_{5p} \quad 0$$

$$0 \quad 0 \quad Y_{5y}$$

$$Y_{5i} = \left[\frac{3}{2} P_i i_{di} \dot{q}_i, \frac{3}{2} P_i \dot{q}_i, \frac{3}{2} P_i^2 i_{qi}^2 \dot{q}_i, \frac{3}{2} P_i^2 i_{di}^2 \dot{q}_i, \right.$$

$$\left. \frac{3}{2} P_i^2 i_{di} \dot{q}_i, \frac{3}{2} P_i^2 \dot{q}_i \right]$$

$$3 P_r i_{qr} u_{dr} / 2 \quad 0 \quad 0$$

$$Y_6 = 0 \quad 3 P_p i_{qp} u_{dp} / 2 \quad 0$$

$$0 \quad 0 \quad 3 P_y i_{qy} u_{dy} / 2$$

$$\frac{3}{2} i_{dr} P_r u_{qr} \quad 0 \quad 0$$

$$Y_7 = 0 \quad \frac{3}{2} i_{dp} P_p u_{qp} \quad 0$$

$$0 \quad 0 \quad \frac{3}{2} i_{dy} P_y u_{qy}$$

$$\frac{3}{2} P_r u_{qr} \quad 0 \quad 0$$

$$Y_8 = 0 \quad \frac{3}{2} P_p u_{qp} \quad 0$$

$$0 \quad 0 \quad \frac{3}{2} P_y u_{qy}$$

4. $Y_1 \sim Y_8$ for the single-axis motion system are

$$Y_1 = i_d$$

$$Y_2 = i_q P \dot{q}$$

$$Y_3 = \dot{i}_d - I_1 (i_d - i_d)$$

$$Y_4 = 2 I_2 \ddot{\tilde{q}} + \ddot{q}_{r1}$$

$$Y_5 = \left[\frac{3}{2} P_i i_{di} \dot{q}_i, \frac{3}{2} P_i \dot{q}_i, \frac{3}{2} P_i^2 i_{qi}^2 \dot{q}_i, \frac{3}{2} P_i^2 i_{di}^2 \dot{q}_i, \frac{3}{2} P_i^2 i_{di} \dot{q}_i, \frac{3}{2} P_i^2 \dot{q}_i \right]$$

$$Y_6 = 3 P_i i_{qr} u_{dr} / 2; Y_7 = \frac{3}{2} i_{dr} P_r u_{qr}; Y_8 = \frac{3}{2} P_r u_{qr}$$

5. Parameters of the single-axis motion system are

$$a_1 = R, a_2 = L_q, a_3 = L_d, a_4 = J$$

$$a_{51} = \left(\frac{L_q}{L_d} - \frac{L_d}{L_q} \right) R, a_{52} = \frac{I}{L_q} R$$

$$a_{53} = \frac{(L_d - L_q)}{L_d} L_q, a_{54} = \frac{(L_d - L_q)}{L_q} L_d$$

$$a_{55} = \frac{(2L_d - L_q)}{L_q} I, a_{56} = \frac{I^2}{L_q}$$

$$a_6 = \frac{(L_d - L_q)}{L_d}, a_7 = \frac{L_d - L_q}{L_q}, a_8 = \frac{I}{L_q}$$

REFERENCES

- [1] Frangos, C., "Control system analysis of a hardware-in-the-loop simulation," *Aerospace and Electronic Systems, IEEE Trans.*, Vol. 26 4, July 1990, pp. 666-669
- [2] Ptak, A. and Foundy, K., "Real-time spacecraft simulation and hardware-in-the-loop testing," *Real-time Technology and Applications Symposium, 1998, Proceedings. Fourth IEEE.* 1998, pp.230-236,
- [3] Ramaswamy, S., Prasad, B.V., Mahajan, R.C. and Goel, P.S., "The role of hardware in-loop motion simulation for Indian satellites," *Aerospace and Electronic Systems, IEEE Trans.*, Vol.27.2, March 1991, pp. 261-267
- [4] Jean-Jacques E. Slotine and Weiping Li. *Applied nonlinear control.* Englewood Cliffs, N.J. Prentice Hall, c1991.
- [5] Riccardo Marino, Patrizio Tomei. *Nonlinear control design: geometric, adaptive, and robust.* London, New York: Prentice Hall c1995.
- [6] In-Cheol Baik, Kyeong-Hwa Kim and Myung-Joong Youn, "Robust nonlinear speed control of PM synchronous motor using boundary layer integral sliding mode control techniques," *Control Systems Technology, IEEE Trans.*, Vol. 81, Jan. 2000, pp. 47-54
- [7] Iwasaki, M., Shibata, T. and Matsui, N., "Disturbance-observer-based nonlinear friction compensation in table drive system," *Mechatronics, IEEE/ASME Trans.*, Vol. 4. 1, March 1999, pp. 3-8.
- [8] Faa-Jeng Lin, Sheng-Lyin Chiu and Kuo-Kai Shyu, "Novel sliding mode controller for synchronous motor drive," *Aerospace and Electronic Systems, IEEE Trans.* Vol. 34. 2, April 1998. pp. 532-542
- [9] Bogosyan, O.S., Gokasan, M. and Jafarov, E.M., "A sliding mode position controller for a nonlinear time-varying motion control system," *Industrial Electronics Society, 1999. IECON '99 Proceedings, the 25th Annual Conference of the IEEE*, Vol. 2, pp. 1008-1013.
- [10] Hacc, A., Jezernik, K., Curk, B. and Terbuc, M., "Robust motion control of XY table for laser cutting machine," *Industrial Electronics Society, IECON'98. Proceedings of the 24th Annual Conference of the IEEE*, Vol. 2, 1998, Pp. 1097-1102.
- [11] Weiping Li and Xu Cheng, "Adaptive high-precision control of positioning tables-theory and experiments," *Control Systems Technology, IEEE Trans.*, Vol. 3, Sept. 1994, pp. 265-270
- [12] Faa-Jeng Lin and Yueh-Shan Lin. "A robust PM synchronous motor drive with adaptive uncertainty observer," *Energy Conversion, IEEE Trans.*, Vol. 14. Dec. 1999, pp. 989-995
- [13] William E. Wiesel. *Spaceflight Dynamics.* International ed. New York. McGraw-Hill. 1992.